# Electrodegradation of tetracycline using stainless steel net electrodes: Screening of main effective parameters and interactions by means of a two-level factorial design

**Maryam Foroughi\*, Hamid Reza Soheil Arezoomand\*, Ali Reza Rahmani\*\*, Ghorban Asgari\*\*\*, Davood Nematollahi\*\*\*\*, Kaan Yetilmezsoy\*\*\*\*\*, and Mohammad Reza Samarghandi\*,†**

\*Department of Environmental Health Engineering, School of Health,
Hamadan University of Medical Sciences, Hamadan, Iran
\*\*Department of Environmental Health Engineering & Research Centre for Health Sciences,
School of Public Health, Hamadan University of Medical Sciences, Hamadan, Iran
\*\*\*Social Determinants of Health Research Center (SDHRC), Faculty of Public Health,
Department of Environmental Health Engineering, Hamadan University of Medical Sciences, Hamadan, Iran
\*\*\*\*Faculty of Chemistry, Bu-Ali-Sina University, Hamadan, Iran
\*\*\*\*\*Department of Environmental Engineering, Faculty of Civil Engineering,
Yildiz Technical University, Davutpasa Campus, 34220, Esenler, Istanbul, Turkey
(*Received 29 May 2017 • accepted 2 August 2017*)

**Abstract**−Performance of electrodegradation process using stainless steel net electrodes was explored for removal of tetracycline (TC) from synthetic wastewater in a laboratory batch study. Main effects of various operating parameters, such as initial TC concentration (20 and 100 mg/L), reaction pH (3.0 and 9.0), current density (4.1 and 17.1 mA/cm$^2$), agitation speed (250 and 750 rpm), and electrolysis time (20, 50, and 80 min), and their interactions on the TC removal efficiency, were optimized by means of a five-factor and two-level factorial experimental design methodology. The significance of responses obtained from the proposed design (sixteen experimental runs under batch mode conditions) was statistically evaluated by preparing a Pareto chart, half-normal probability plot, and plots of main effects and their interactions (herein referred to as Factions) within the framework of the analysis of variance (ANOVA). The statistical results corroborated with 95% certainty that TC concentration, pH, and current density showed the largest effects (absolute values) on the TC removal efficiency. Besides the most effective Factions, a sodium sulfate (used as supporting electrolyte) dose of 1 g/200 cc was determined as the optimum value for the studied process. Under the conditions of an initial TC concentration=20 mg/L, a reaction pH=3.0, current density=17.1 mA/cm$^2$, an agitation speed=250 rpm, and an electrolysis time=20 min, about 70% of TC could be successfully removed from the simulated wastewater. Findings of this experimental study clearly confirmed the applicability of the electrodegradation process for the removal of a broad spectrum antibacterial agent like TC, and also demonstrated the effectiveness of the factorial design methodology before transferring the obtained experimental knowledge for a full-scale facility.

Keywords: Electrodegradation, Screening, Factorial Experimental Design, Stainless Steel Nets, Supporting Electrolyte, Tetracycline

## INTRODUCTION

As a group of powerful medicines in therapy of infectious diseases, antibiotics have been widely used worldwide for both humans and animals. However, in recent years, these compounds have also been regarded as emerging environmental contaminants under the class of pharmaceuticals and personal care products (PPCPs) [1]. Extensive and inappropriate use of antibiotics causes intensive releasing of them into wastewater treatment facilities (WWTFs), since they are not metabolized or absorbed completely in the body of human or livestock [2,3]. On the other hand, inadequate re-

moval of pharmaceutical compounds in conventional WWTFs leads to their continuous release into the environment through various pathways such as wastewater effluents, sludge, and even agricultural runoff [4,5].

Tetracycline (TC) is a broad spectrum antibacterial agent which has been ranked as the second worldwide antibiotic in both production and usage for human therapy, veterinary medicine, and aquaculture [6-8]. However, about 80-90% of the administered TC is excreted into aquatic ecosystems due to poor absorption, low metabolism, misuse, and overuse [9,10]. Since the presence of antibiotics can alter microbial metabolism and diversity, TC occurrence is suspected to have hazardous impacts on both human health and environment due to risks associated with the uncontrolled discharge of antibiotics [11]. The terrible consequences, such as dissemination of antibiotic resistance genes (which can no longer be treated

with the presently known drugs) due to the ineffectiveness of conventional treatment systems, has led to the requirement for investigation of efficient and cost-effective approaches for treatment of TC-containing wastewater [8,12].

Due to increasing environmental awareness coupled with more stringent regulation standards, various industries challenge themselves in seeking appropriate wastewater treatment technologies [13], including the degradation of TC. Among various technologies for degradation of TC, electrochemical technology offers many distinctive advantages in terms of versatility, high energy efficiency, safety, amenability of automation, and cost effectiveness [14]. Moreover, growing attention has been paid to the advanced oxidation processes (AOPs) for the removal of TC from aqueous systems [15]. Comparatively, electrochemical advanced oxidation processes (EAOPs) have gained more attention in recent years, since they are environmentally clean [16], and use electrons as a reagent in complete mineralization of TC [17]. EAOPs are mainly based on producing hydroxyl radicals (OH$^{\bullet}$) as very powerful oxidants which are capable of oxidizing a wide range of organic compounds [18].

In AOP-based systems, different materials, such as $IrO_2$, $PbO_2$, boron-doped diamond (BBD), iron, and stainless steel (SS), have been investigated as electrode materials [18]. Among them, metal-like materials (i.e., SS) show a sufficiently high electric conductivity and good inoxidizability. They are also comparatively inexpensive and easy to process and assemble, so these materials are well suitable for scaling-up [19]. Electrocoagulation (EC) with SS electrodes has been reported superior to its counterpart with iron electrodes from both technical and economic point of views [20].

Many factors including current density, electrolysis time, initial concentration, and reaction pH, etc., can influence the pollutant removal in an electrochemical process [21,22]. But more importantly, detection of the statistically significant factors is the first consideration that should be taken into account [23]. Screening the most influential factors is also the primary objective of an experimental design for a specific process. This type of design is very useful to evaluate qualitative, quantitative, and mixed parameters simultaneously [24]. For this reason, factorial design of experiments (DOE) offer several advantages over the traditional one-factor-at-a-time (OFAT) methods for statistically screening procedure. For example, two-level factorial designs are capable of estimating the main effects of individual factors, as well as their interaction effects (herein the is effect of factors and interactions simply referred to as "Factions") with only a few experimental runs. The effect of more contributing parameters can be investigated by using these factors (i.e., at a time, 15 individual factors) for screening and finding the significant ones. Moreover, the statistical power (the precision of effect estimation) is considerably enhanced, allowing for a broader generalization of the results [25,26].

Although the experimental design methodology has been widely studied as an effective technique to understand the associations between various process-related variables [27-31], to the best of the authors' knowledge, almost no papers have been published to date regarding the screening main effective parameters and their interactions (Factions) on the removal of TC from wastewater by an electrochemical process using stainless steel nets as the reactor electrodes. Thus, to clarify the place of this subject and to fulfill the

relevant gap in the scheme of the experimental design procedure, we focused on a cost-effective strategy exploring the best operating conditions of TC removal for wastewater treatment plants. For this aim, a detailed experimental design methodology (five-factor, two-level) was implemented for determining the Factions of initial TC concentration, reaction pH, current density, agitation speed, and electrolysis time on the TC removal by using stainless steel nets serving as the electrode material.
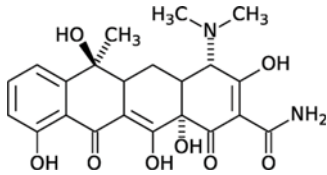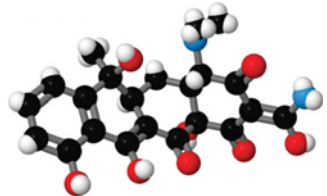
## MATERIALS AND METHODS

### 1. Chemicals and Analytical Procedure

All chemicals used were of analytical reagent grade, and no further purification was needed before analysis. Tetracycline (TC) with chemical formula $C_{22}H_{24}N_2O_8 \cdot xH_2O$ (purity ≥98%) was purchased from Sigma Aldrich (St. Louis, MO, USA), and its characteristics are summarized in Table 1 [32]. $Na_2SO_4$ (Sodium Sulfate Anhydrous for Analysis EMSURE® ISO, product code: 1.06649.1000, Merck-Millipore, USA) was used as the supporting electrolyte (SE) in predetermined concentration of 1 g/200 cc.

For each experiment run, a synthetic TC-containing wastewater was prepared using tetracycline powder. Simulated wastewater provides more reproducible experimental conditions, and consistent characteristics than real wastewater, and is required to obtain a reliable kinetic database [33,34]. After adjusting all components of the freshly prepared solution, samples were colllected at predetermined time intervals by passing through 0.45 μm membrane filter, and measured for the final TC content by using a spectropho-

**Table 1. Tetracycline chemical structure and its related information**

| Component | Information/schematic/value |
| --- | --- |
| Compound | Tetracycline |
| Molecular (chemical) formula | $C_{22}H_{24}N_2O_8 \cdot xH_2O$ |
| 2D structure |  |
| 3D structure |  |
| Molecular weight (g/mol) | 444.435 (anhydrous basis) |
| $\lambda_{max}$ (maximum wavelength, nm) | 359 |
| $pKa_1$ ($\alpha$-carboxyl group) | 3.3 |
| $pKa_2$ ($\alpha$-ammonium ion) | 7.7 |
| $pKa_3$ (side chain group) | 9.7 |
| Physical Form | Crystalline powder |
| Appearance | Pale yellow |
| Melting point | 172-174 °C |
| Storage temperature | 2 to 8 °C |

tometer (model 1700, HACH, USA) at a wavelength of 372 nm. This was employed after scanning (between 200 and 800 nm) at different TC concentrations with $R^2$=0.9987. The measurements' accuracy was then assessed by a high performance liquid chromatography, HPLC Agilent 1260 infinity (Agilent Technologies Co. Ltd., USA) equipped with a Shimadzu LC-20 AB pump (dimensions (H×W×D): 140 mm×260 mm×420 mm, weight: 10 kg, operating temperature range: 4-35 °C, power requirements: 100 VAC, 150 VA, 50/60 Hz, maximum discharge pressure: 40 MPa, flow-rate setting range: 0.0001 to 10.0000 mL/min, solvent delivery method: parallel-type double plunger, plunger capacity: 10 μL), a Shim-Pack VP-ODS-C18 column (dimensions: 4.6 mm I.D.×250 mm L.×5 μm, particle size: 5 μm, pore size: 12 nm, surface area: 410 m$^2$/g, carbon loading: 20%, pressure tolerance: ~20 MPa, pore volume: 1.25 mL/g, pH range: 2-7.5, bonding type: monomeric), and a UV-Vis spectrophotometer (Shimadzu UV-1600 (Japan), dimensions (H×W× D): 380 mm (200 mm at closing LCD unit)×550 mm×470 mm, weight: 18 kg, power consumption: 160 VA, frequency: 50/60 Hz, wavelength range: 190 to 1,100 nm, wavelength accuracy: ±0.5 nm, wavelength repeatability: ±0.1 nm, photometric range: absorbance: −0.5 to +3.999 Abs, photometric accuracy (at 0.5 Abs): ±0.002 Abs, photometric repeatability (at 0.5 Abs): ±0.001 Abs). A mixture of methanol (CH$_3$OH) and water (H$_2$O) (50 : 50 v/v, HPLC grade, Merck) was passed at flow rate of 1 mL/min at 25 °C as the mobile phase. A 20 μL of TC solution (1-20 mg/L) was injected into the column at a retention time of 3.6 min and then measured at a fixed wavelength of 359 nm. Additional measurement details (HPLC calibration curve, spectrophotometer calibration curve, and correlation between HPLC and spectrophotometer concentrations) are presented in the Supplementary Information (SI) (Figs. S1-S3). TC removal efficiency was computed using the following equation:

$$\% \text{ TC removal} = \left( \frac{\text{TC}_i - \text{TC}_t}{\text{TC}_i} \right) \times 100 \qquad (1)$$

where, $\text{TC}_i$ and $\text{TC}_t$ represent the initial and final concentrations of TC (mg/L), respectively. The solution pH was adjusted using 0.1 M HNO$_3$ (Nitric Acid 65% for Analysis EMSURE® ISO, product code: 1.00456.2500, Merck-Millipore, USA) or 0.1 M NaOH (Sodium Hydroxide Pellets Gr for Analysis EMSURE® ISO, product code: 1.06498.5000, Merck-Millipore, USA), and measured off-line by using a portable pH/mV/temperature meter (HACH model sension1 (USA), dimensions (H×W×D): 21.2 cm×8.7 cm× 4.2 cm, weight: 0.3 kg, 0.2 mV or ±0.01% of reading, ±0.3 from 0-70 °C; ±1.0 from >70-110 °C).

## 2. Experimental Setup and Protocol

The experimental reactor consisted of a cube Plexiglas cell having a total and a working volume of 250 mL and 200 mL, respectively. Two stainless steel nets (purchased from a local market) in dimensions of 4.5 cm×6.5 cm were used as both anode and cathode electrodes, and were immersed in parallel with a fixed distance of 5 cm. Current was supplied by a direct current (DC) power source (DAZHENG PS-305D (China), dimensions (H×W×D): 275 mm×128 mm×162 mm, weight: 4.4 kg, voltage: 0-30 V, electric current: 0-5 A, working condition temperature: −10-40 °C, permissible relative humidity: <90%, voltage stability: <0.01% +2 mV). All batch experiments were performed at room temperature in
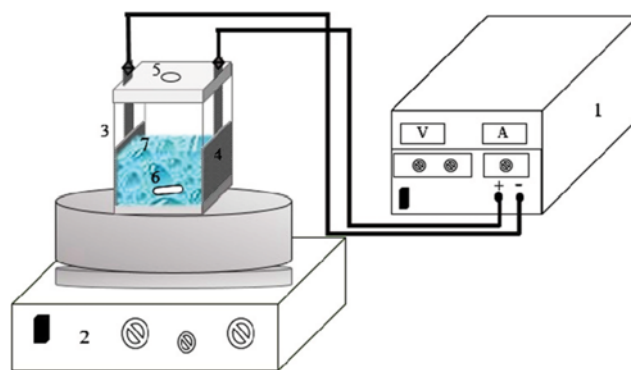


**Fig. 1. Schematic diagram of the electrochemical reactor.**

| | |
|---|---|
| 1. Power supply | 5. Sampling port |
| 2. Magnetic stirrer | 6. Magnetic stirring bar |
| 3. Electrochemical cell | 7. Simulated tetracycline (TC) |
| 4. Stainless steel net | solution |
| electrodes | |

duplicate. The experimental setup is shown in Fig. 1.

For each experiment, 200 cc of freshly prepared TC solution was subjected to electrochemical process after adjusting its pH, adding 1 g Na$_2$SO$_4$, and applying desired agitation speed, which was assured by a hotplate magnetic stirrer (Alfa, HS-860, (Tehran, Iran), dimensions (H×W×D): 120 mm×200 mm×200 mm, weight: 2.8 kg, setup plate dimension: Ø175 mm, minimum and maximum stirring bar lengths: 20 mm and 80 mm, speed range: 100-1,800 rpm, heating temperature range: 50-300 °C, permissible ambient temperature: 5-40 °C, permissible relative humidity: 80%, voltage: 230 V, frequency: 50/60 Hz, power input: 665 W). The samples were collected at three electrolysis times of 20, 50, and 80 min from about 5 cm below the solution surface for the further analyses.

## 3. Performance Stability of Electrodes

The performance stability of electrodes was tested before the screening experiments in order to detect possible electrolysis times to use the electrodes without any significant influence on the process efficiency. For this purpose, 12 experiments under TC concentration=100 mg/L, pH=7.0, agitation speed=520 rpm, and current density=10.25 mA/cm$^2$ were performed. Each two experiments were considered as a separate treatment category, and its significance was investigated in comparison to other categories (see Table 3).

## 4. Optimum Concentration of the Supporting Electrolyte (SE) Dose

Electrolyte improves the solution conductivity, accelerates the electron transfer, and thereby enhances the performance of the electrochemical reaction. Therefore, determination of SE dose is necessary to improve the ionic strength especially for the solutions without enough conductivity [35,36]. To find the optimum concentration of the SE dose, which could provide the studied current density (4.1-17.1 mA/cm$^2$), various concentrations of sodium sulfate (Na$_2$SO$_4$) (0.2-1.0 g) were dissolved in 200 cc TC solution, and the corresponding potential was then assessed after applying the currents.

## 5. Strategy of Study

Screening designs are mainly applied to identify the significant

**Table 2. Experimental ranges and levels of parameters**

| Symbol | Factor name | Unit | Ranges and levels | | |
| --- | --- | --- | --- | --- | --- |
| | | | Low level (−1) | | High level (+1) |
| A | TC concentration | mg/L | 20 | | 100 |
| B | pH | - | 3.0 | | 9.0 |
| C | Current density (CD) | mA/cm$^2$ | 4.1 | | 17.1 |
| D | Agitation speed | rpm | 250 | | 750 |
| | | | Low (−1) | Medium (0) | High (+1) |
| E | Time (T) | min | 20 | 50 | 80 |

Factions (effects and interactions) among a large number of parameters [37]. A two-level factorial design is an appropriate approach to estimate the main Factions in which each independent factor is studied over two coded levels of (−1) and (+1) referred as high and low level, respectively [37]. In this study, the effects of four variables, namely TC initial concentration, pH, current density, and agitation speed in three times (20, 50, and 80 min) were investigated for screening of main effective Factions for the present process. The ranges and level of the parameters are presented in Table 2. The ranges of the model variables were chosen in accordance with the relevant literature [6,38-46].

The variables were selected based on the previous reports on TC degradation using electrochemical-based processes [45,46]. Moreover, in selection of time intervals from preliminary studies, the TC removal efficiency increased from 20 min, and then it turned into a flat trend after 80 min. Therefore, this range was considered as the operating range for the present case. Both design of experiments and data analysis were conducted using Minitab v.17 (Minitab Inc., State College, PA, USA) and Design Expert 7.0.0 (Stat-Ease, USA) software packages.

**Table 3. Comparative performance of the electrodes for different treatment categories**

| Run | TC removal efficiency (%) | Treatment category | Comparison | Prob>\|t\|[a] |
| --- | --- | --- | --- | --- |
| 1 | 47.20 | | 1 vs 2 | 0.5517 |
| 2 | 47.09 | 1 | 1 vs 3 | 0.0366 |
| | | | 1 vs 4 | 0.0003 |
| 3 | 46.98 | | 1 vs 5 | <0.0001 |
| 4 | 46.46 | 2 | 1 vs 6 | <0.0001 |
| | | | 2 vs 3 | 0.0864 |
| 5 | 46.12 | 3 | 2 vs 4 | 0.0005 |
| 6 | 44.58 | | 2 vs 5 | <0.0001 |
| 7 | 42.85 | | 2 vs 6 | <0.0001 |
| 8 | 41.59 | 4 | 3 vs 4 | 0.0034 |
| 9 | 37.08 | | 3 vs 5 | <0.0001 |
| 10 | 36.06 | 5 | 3 vs 6 | <0.0001 |
| 11 | 35.30 | | 4 vs 5 | 0.0006 |
| 12 | 35.01 | 6 | 4 vs 6 | 0.0046 |
| | | | 5 vs 6 | 0.0787 |

[a]P-values (associated with a two-tailed test) <0.05 were considered to be significant

## RESULTS AND DISCUSSION

### 1. Performance Stability

As can be seen from both Table 3 and corresponding Fig. 2, comparisons of all treatment categories showed that the performance significantly reduced after four times ($p$-value=0.0366<$\alpha$=0.05). Thus, insignificant Prob>\|t\| for category 1 versus 2 indicated that the electrodes could be used for four times without any significant effect on the system performance. Therefore, in further experiments, the electrodes were replaced with new ones after four times application.

### 2. Effect of Na$_2$SO$_4$ Concentration

Selection of the optimum sodium sulfate (used as supporting electrolyte, SE) dose is based on the appropriate applied voltage which is directly proportional to energy consumption and operational cost. As seen from Table 4, all concentrations could provide the required current densities, but higher potentials need to be applied at low SE doses. Since the addition of SE imposes less costs than applying higher potential, and the real wastewater has enough conductivity inherently, therefore, a higher SE dose sounds to be less controversial than applying a higher potential. Consequently, a supporting electrolyte dose of 1 g/200 cc was selected as the opti-
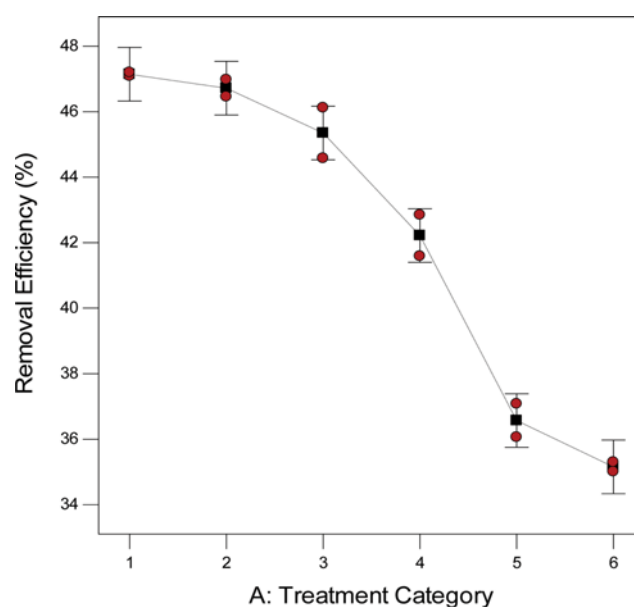


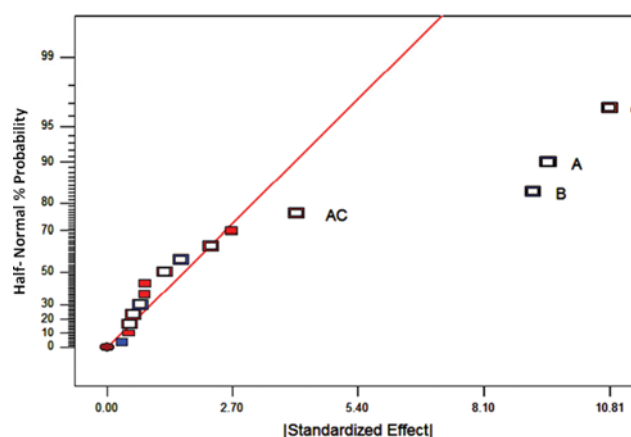**Fig. 2. One-factor graph showing the effect of electrode performance.**

**Table 4. SE doses providing desired currents and the corresponding potentials**

| SE dose (g/200 cc) | Current (A) | Voltage (V) |
|---|---|---|
|     | 0.03 | 4.5 |
| 0.2 | 0.07 | 9 |
|     | 0.45 | 42.3 |
|     | 0.03 | 3.8 |
| 0.3 | 0.07 | 7.3 |
|     | 0.45 | 31.4 |
|     | 0.03 | 3.6 |
| 0.5 | 0.07 | 5.3 |
|     | 0.45 | 22 |
|     | 0.03 | 3 |
| 1.0 | 0.07 | 3.9 |
|     | 0.45 | 12.4 |



**Fig. 3. Half-normal probability plot showing effects of parameters and their interactions (Factions) on the TC removal efficiency ($\alpha=0.05$).**

mum value for the present case.

**3. Screening of Main Effective Factions**

In this study, a two-level experimental design methodology was applied for screening of the main effective Factions. The design matrix, which consisted of sixteen experimental runs conducted under batch conditions, and the obtained responses are summarized in Table 5. The normality of obtained responses was evaluated using Anderson-Darling test ($p$-value=$0.23 > \alpha = 0.05$). There are some interpreting plots for determination of main effective Factions, one of which (and maybe the most valuable one) is the half-normal probability plot. In this graph, a guide line divides the space into two sections, in which the most effective parameters appear in the upper right part, while parameters and interactions (Factions) having a small or noise effect are illustrated on the left part [47]. For the present case, the plot of half-normal probability (introduced by Cuthbert Daniel in 1959) is depicted in Fig. 3. This

plot shows the magnitude (from smallest to largest) of the effects of factors (individual variables and their interactions) as standardized effects along the $x$-axis. The standardized effect for a factor can be expressed as the difference of the average response variable over high factor levels minus the average response over the low factor levels. The values on the $y$-axis are defined by the idealized expected values for the number of effects, ranked by increasing value, if drawn from a half-normal distribution [48]. Thus, the $y$-value for the $j$th effect is the half-normal probability value for the $j$th value (rank) in a variable with $N$ observations. A half-normal distribution is the distribution of the abs($X$) with $X$ having a normal distribution with mean zero. The absolute value of a factor's effects is the value plotted on the $x$-axis, but the color of the data points indicates whether the original effect is positive (red) or negative (blue). The points comprising factors with small and/or insignificant effects on the response will describe (roughly) a straight line

**Table 5. Design matrix and the corresponding responses**

| Standard order | Run | TC concentration (mg/L) | pH | CD (mA/cm$^2$) | Agitation speed (rpm) | TC removal efficiency (%) T=20 min |
|---|---|---|---|---|---|---|
| 1 | 3 | 20 | 3.0 | 4.1 | 250 | 59.18 |
| 2 | 8 | 100 | 3.0 | 4.1 | 250 | 46.16 |
| 3 | 5 | 20 | 9.0 | 4.1 | 250 | 49.26 |
| 4 | 9 | 100 | 9.0 | 4.1 | 250 | 35.61 |
| 5 | 16 | 20 | 3.0 | 17.1 | 250 | 68.38 |
| 6 | 1 | 100 | 3.0 | 17.1 | 250 | 58.19 |
| 7 | 10 | 20 | 9.0 | 17.1 | 250 | 58.28 |
| 8 | 6 | 100 | 9.0 | 17.1 | 250 | 54.92 |
| 9 | 12 | 20 | 3.0 | 4.1 | 750 | 61.53 |
| 10 | 2 | 100 | 3.0 | 4.1 | 750 | 50.29 |
| 11 | 15 | 20 | 9.0 | 4.1 | 750 | 51.51 |
| 12 | 4 | 100 | 9.0 | 4.1 | 750 | 35.14 |
| 13 | 14 | 20 | 3.0 | 17.1 | 750 | 66.66 |
| 14 | 11 | 100 | 3.0 | 17.1 | 750 | 58.20 |
| 15 | 7 | 20 | 9.0 | 17.1 | 750 | 55.08 |
| 16 | 13 | 100 | 9.0 | 17.1 | 750 | 55.42 |

on the plot. The points for factors with a large and significant effects will visually fall off of the straight line described by the insignificant factors. A red line of the insignificant factors helps to graphically describe the difference between significant and insignificant factors. Therefore, selecting the factor points which displace well off of the line describing insignificant factors is the most important task of the half-normal probability plot to identify important factors and start the process of optimizing the model [49]. Based on the above-noted facts, parameters of A, B, and C, as well as interaction of AC, have significant effect on the electrochemical degradation of TC using stainless steel net electrodes (Fig. 3). More specifically, the individual parameters A, B, C have the largest effects (absolute values) on the TC removal efficiency as compared to interaction term of AC, since these parameters appear in the upper-right section of the half-normal plot [50].

Another useful plot for identifying of Factions is the Pareto chart as a graphical representation of the analysis of variance (ANOVA) test, where $t$-value is based on the determination of any remaining Factions' effect. Pareto plot bars represent the standardized effects of each involved parameters in descending order of contribution to the output of the process [51]. The red bars indicate a positive effect of its own Faction, while blue bars show negatively affecting Factions. The Pareto chart of this study (Fig. 4) shows

that the effects of A and B are negative, while the independent factor C and the interaction term AC have positive effects on the process because the $t$-value of the mentioned factions exceeds the limit of 2.571 (the $p$-value was set at 0.05). Additionally, the parameters A, B, and C exceed another limit called the Bonferroni limit line ($t$-value of effect=5.247), which cuts into half the $p$-value of 0.05 to a much stricter level of 0.025 [48]. Coefficients with $t$-value of effect above Bonferroni limit line are designated as certainly significant, and coefficients with $t$-value of the effect between Bonferroni line and $t$-value limit line are termed as possibly significant, while coefficients with $t$-value of effect below the $t$-value limit line are statistically insignificant and should be removed from the analysis [50,52]. On the basis of the foregoing facts, it can be concluded from the Pareto chart that the independent factors A, B, and C have shown certainly significant effects towards the system, and the two factor interaction of AC has shown an intermediate (or possibly significant) effect. Furthermore, other factors (i.e., BC, CD, AB, BD, AD, D) should be excluded from the the present analysis, since their $t$-values of effect are observed below the $t$-value limit line.

Interactions, regardless the effect of their components indivisibly, can be categorized to synergisms or antagonisms [53]. In this study, for example, a synergistic effect was estimated for interac-
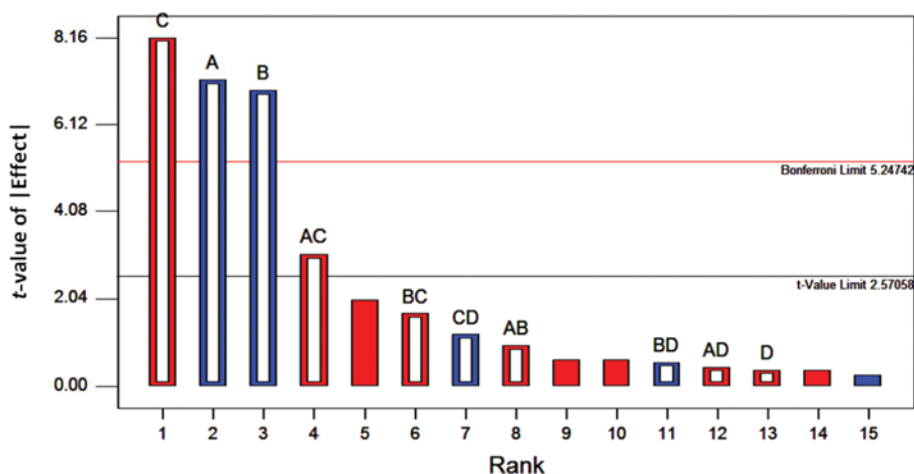


Fig. 4. Pareto chart of the main effects obtained from the screening experiments.
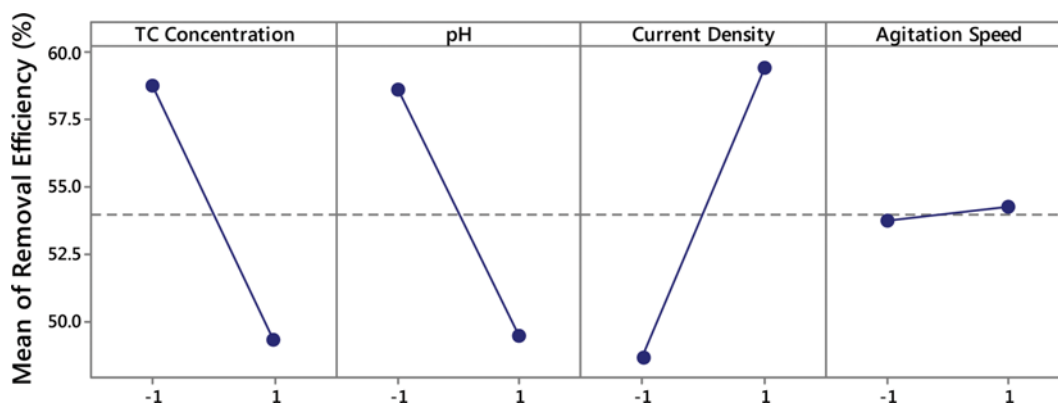


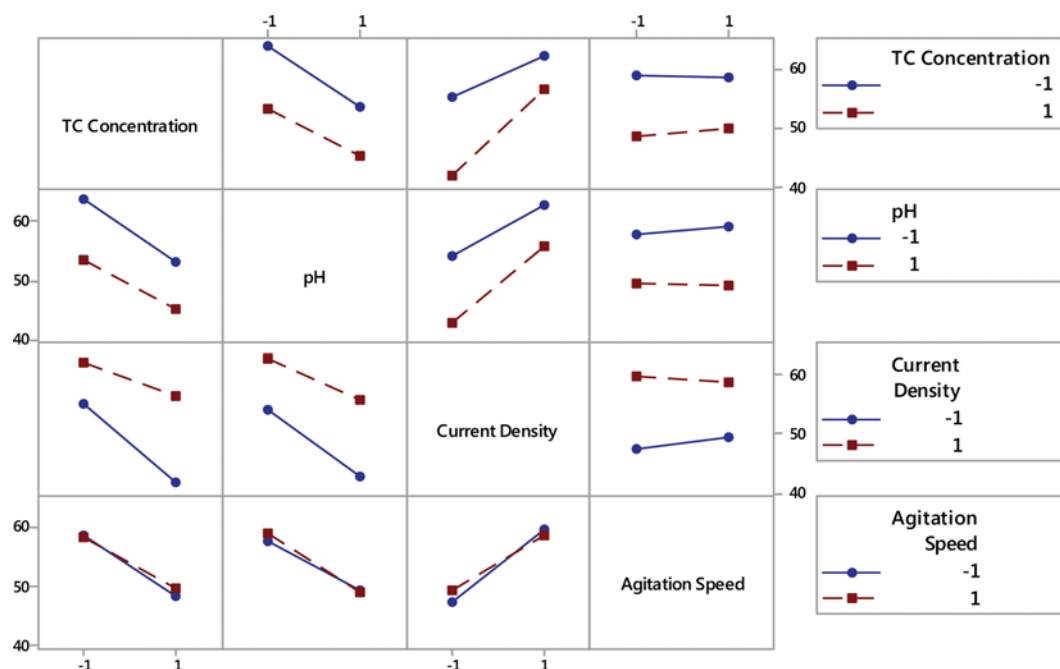Fig. 5. Main effects plot of contributed parameters.

**Fig. 6. Interactions plots of Factions in TC removal.**

tion of AC, while a negative effect for A and a positive effect for C was introduced, respectively. The magnitude and trend of all factors contributed on the process can be illustrated by the main effect plot which is depicted in Fig. 5. In this plot, the influence of each contributed parameter (while others are assumed constant) is individually assessed in terms of their slope, trend, and magnitude. Fig. 5 shows that agitation speed has a small effect on the process due to having a low magnitude in addition to low slope versus horizontal gridline, while other three Factions' effects are more sensible, and the effect of the current density is even much more among them. The patterns' statistical significance was also checked by ANOVA, and $p$-values of 0.0008, 0.001, 0.0004, and 0.027 were extracted for the parameters of A (TC concentration), B (pH), C (current density), and AC, respectively.

As mentioned, the depicted effect on Fig. 6 only shows magnitude, trend, and importance of a given factor, without considering concomitant effects between parameters contributed. This limitation would be overcome by using an interaction plot, in which interaction among the factors could be visualized. Indeed, an interaction may occur when the change in response (as dependent variable) from the low level to high level of a variable is not similar to the change in the response at the same two levels of a second variable. In other words, the effect of one factor depends on the level of the another factor [54].

Parallel lines in an interaction plot indicate no interaction, and, vice versa, any departure from parallel trend could be attributed to an interaction effect. In fact, the greater difference in slope between the lines indicates a higher degree of interaction. However, this plot is not able to identify whether the interaction is statistically significant. Since interaction plots are most often used to visualize interpreted interactions during ANOVA or DOE, their meaningfulness can be addressed using ANOVA [55]. As is visible from Fig. 6 that
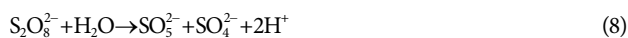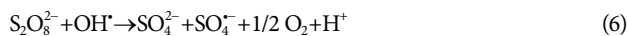
two lines between TC and current density departure from the parallel indicates their interaction effect, whose significance was also confirmed by ANOVA ($p$-value of $0.027 < \alpha = 0.05$).

**4. Influence of Factions on Electrodegradation Process**

With investigation of three times (20, 50, and 80 min) on TC removal by the electrochemical process, it was determined that although a slight increment in the removal efficiency as the reaction time was increased (data not shown), but the electrolysis time of 20 min was selected for some operational reasons, including the fact that energy consumption and subsequent operation costs at higher time increased progressively [20]. Also, development of red to brown color in the solution as a health and aesthetics-based challenges at higher times was another reason for selecting of the optimum time of 20 min. On the other hand, the electrolysis time below the optimum time of 20 min (i.e., electrolysis times of 5, 10, and 15 min) showed statistically lower efficiencies ($p=0.0466$ for 15 and 20 min, data were not shown). This can be attributed to insufficient contact time for producing of oxidation agents and decomposation of TC ions, which subesquently causes incomplete degradation and mineralization of other recalcitrant organic pollutants that consume most of the current applied in the electrooxidation process [40,56].

When the sodium sulfate ($Na_2SO_4$) is used as supporting electrolyte (SE) for rising the electrical conductivity of the solution (which in turn led to higher current density), the indirect oxidation by the hydroxyl radicals ($OH^\bullet$) (Eq. (5) and the the sulfate radicals ($SO_4^{\bullet-}$) (Eqs. (2), (4), and (6)) can take place during the electrolysis process. The following equations are the summarized reactions of the formation of oxidizing species such as peroxydisulfate or persulfate ($S_2O_8^{2-}$) (Eq. (9)) and hydrogen peroxide ($H_2O_2$) (decomposition of peroxydisulfate ion to $O_2$ (Eq. (6), to bisulfate ion ($HSO_4^-$) (Eq. (7)), to peroxymonosulfate (or monopersulfate) ion

$(SO_5^{2-})$ (Eq. (8), and further to $H_2O_2$ (Eq. (9)) [51,57-59]:

$$SO_4^{2-} \rightarrow SO_4^{\cdot-} + e^- \tag{2}$$

$$SO_4^{\cdot-} + SO_4^{\cdot-} \rightarrow S_2O_8^{2-} \tag{3}$$

$$S_2O_8^{2-} + 2e^- \rightarrow SO_4^{2-} + SO_4^{\cdot-} \tag{4}$$

$$SO_4^{\cdot-} + OH^- \rightarrow SO_4^{2-} + OH^{\cdot} \tag{5}$$

$$S_2O_8^{2-} + OH^{\cdot} \rightarrow SO_4^{2-} + SO_4^{\cdot-} + 1/2\ O_2 + H^+ \tag{6}$$

$$S_2O_8^{2-} + H_2O \rightarrow 2HSO_4^- + 1/2\ O_2 \tag{7}$$

$$S_2O_8^{2-} + H_2O \rightarrow SO_5^{2-} + SO_4^{2-} + 2H^+ \tag{8}$$

$$SO_5^{2-} + H_2O \rightarrow H_2O_2 + SO_4^{2-} \tag{9}$$

Compared to NaCl, $Na_2SO_4$ prevents or minimizes potential risks of organic pollutants from chlorinated organic compound intermediates or even the main products of the electrooxidation-based treatment. Thus, the major disadvantage of NaCl application as SE is that it is susceptive to generating and to accumulating toxic chloroderivatives, trihalomethanes (THMs) and chloramines ($NH_2Cl$), which enhance the toxicity of the treated solution. Furthermore, the additional oxidative nature of active chlorine does not usually result in higher COD (chemical oxygen demand) or TOC (total organic carbon) removal rates compared to those determined for elecrooxidation in sulfate medium, although at least it accelerates the degradation of the initial pharmaceutical and its cyclic/aromatic products, as found for $\beta$-blocker metoprolol [22].

The small effect of mixing speed on the process, which has also been reported by Yehya et al. [60], means that regardless of TC decomposation mechanism, no apparent limitation is imposed by mass transfer in the process. This is a key point because electrooxidation may be controlled by mass transfer, which leads to pseudo-first order kinetics. Therefore, the speed of 250 rpm was finally considered, to prevent swirling in addition to reducing the power input for mixing purpose. In a past study on sulfite oxidation, Wisniak et al. [61] reported that agitation below a certain speed did not have much influence on the reaction rate, and the mixing was not able to break the bubbles in a sufficient manner to create additional area. Additionally, in a recent study on decolorization of distillery spent wash effluent by electrooxidation and Fenton processes, David et al. [38] concluded that a further increase in the agitation speed beyond the optimum value did not have a major effect on the spentwash decolorization. This was attributed to the fact that agitation above a particular speed might cause breaking of flocs and disruption of accumulated organic matter back to the solution, resulting in a decrease in the removal efficiency [62,63].

Influencing TC abatement of by mainly current density suggests that the dominant mechanism in degradation can be attributed to an electro-oxidation reaction [64]. Moreover, the decreasing in removal efficiency by the increase of TC concentration can contribute to the competitive consumption of oxidizing $\cdot$OH radicals between TC antibiotic and generated intermediate compounds, as well as to the total saturation of the electrode surface [65]. Positive effect of AC interaction, which can express that the influence of current density is more pronounced at higher concentrations of TC, is in close agreement with the report of Yahiaoui et al. [65]. Also, the findings could be described by assuming a diffusion control in the electro-decomposition process. Some factors, such as increasing of concentration, can enhance the mass transfer from the bulk of the solution to the electrode's surface and also to the oxidation species in the solution that results in providing more opportunities for TC molecules degradation [6]. The phenomenon appears to be more synergetic in interaction of TC concentration and current density (i.e., AC interaction). In other words, it seems that high concentration of TC along with high current density impose a high gradient favorite for TC exposure with the oxidant species.

Solution pH imposes different charges on surfaces sites of TC. At pH<3.3, the molecule due to the protonation of dimethyl ammonium ($C_2H_8N$) group turns to cation ($TCH^{3+}$), while it converts to a zwitterion form (a neutral molecule with both positive and negative electrical charges) ($TCH_2^0$) at pH 3.3-7.7 due to loss of a proton from the phenolic-diketone moiety. For higher pH (more than 7.7) anion forms of TC would be dominant (in forms of $TCH^-$ or $TC^{2-}$) due to the loss of active protons from the tricarbonyl system and phenolic-diketone moiety [32]. Therefore, at low pH, amino groups of TC would be protonated, hence their reactivity toward the highly nucleophilic hydroxyl radicals will be increased [51]. Positive interaction effect of AC parameter may ascribed to the fact that the effect of current density is more pronounced at higher concentrations of TC. This is in close agreement with the report of Yahiaoui et al. [65].

## CONCLUSION

Although many influential factors have been reported on the electrochemical process, only some of them show a significant effect in real systems. In this work, the main effective Factions on the process were screened by means of a two-level factorial design. All conceivable combinations of the contributing parameters were successfully evaluated within the framework of this well-defined strategy through some valid and powerful analyse,s including Pareto chart, half-normal probability plot, main effects and interaction plots, which were all coupled with ANOVA analysis. The most effective Factions introduced by the studied procedure were found as TC concentration, pH, current density, and the interaction effect of TC concentration and current density. Moreover, some basic conditions such as the optimal value of SE (1 g/200 cc) and stability of the electrodes performance (four times without any significant change in the efficiency at same conditions) were identified. The results showed that when the optimal dose of SE was applied at an initial TC concentration of 20 mg/L, a reaction pH of 3.0, a current density of 17.1 mA/cm$^2$, an agitation speed of 3 rpm, and an electrolysis time of 20 min, about 70% of TC removal could be achieved by the electrochemical process. This study demonstrates the treatability of a broad spectrum antibacterial agent by electrodegradation, and also the usefulness of the experimental design methodology in determining main effects and relationships of the process-related parameters before building and operating of a full-scale system. Consequently, the supportive results of

this study have encouraged the authors to conduct some follow-up work. These future plans can be summarized as follows: (a) modification and upgrading of the proposed process in experimental, bench, and pilot scales, and even for (b) management and scaling-up in the large facilities by working on a three-dimensional electrode system.

## ACKNOWLEDGEMENTS

## SUPPORTING INFORMATION

Additional information as noted in the text. This information is available via the Internet at http://www.springer.com/chemistry/journal/11814.

## REFERENCES

1. H. Zhang, P. Liu, Y. Feng and F. Yang, *Marine Pollution Bulletin*, **73**, 282 (2013).
2. G. Hou, X. Hao, R. Zhang, J. Wang, R. Liu and C. Liu, *Biores. Technol.*, **212**, 20 (2016).
3. S. Rodriguez-Mozaz, S. Chamorro, E. Marti, B. Huerta, M. Gros, A. Sànchez-Melsió, C. M. Borrego, D. Barceló and J. L. Balcázar, *Water Res.*, **69**, 234 (2015).
4. A. Garcia-Rodríguez, V. Matamoros, C. Fontàs and V. Salvadó, *Chemosphere*, **90**, 2297 (2013).
5. L. Hou, H. Zhang and X. Xue, *Sep. Purif. Technol.*, **84**, 147 (2012).
6. C. Brinzila, M. Pacheco, L. Ciríaco, R. Ciobanu and A. Lopes, *Chem. Eng. J.*, **209**, 54 (2012).
7. Q. Yi, Y. Gao, H. Zhang, H. Zhang, Y. Zhang and M. Yang, *Chem. Eng. J.*, **300**, 139 (2016).
8. J. Ou, M. Mei and X. Xu, *J. Solid State Chem.*, **238**, 182 (2016).
9. J. Li, M. Han, Y. Guo, F. Wang, L. Meng, D. Mao, S. Ding and C. Sun, *Appl. Catal. A: Gen.*, **524**, 105 (2016).
10. Q. Liu, Y. Zheng, L. Zhong and X. Cheng, *J. Environ. Sci.*, **28**, 29 (2015).
11. Z. N. Norvill, A. Toledo-Cervantes, S. Blanco, A. Shilton, B. Guieysse and R. Muñoz, *Bioresour. Technol.*, **232**, 35 (2017).
12. X. Zhu, Y. Liu, F. Qian, C. Zhou, S. Zhang and J. Chen, *Bioresour. Technol.*, **154**, 209 (2014).
13. C. Y. Teh, P. M. Budiman, K. P. Y. Shak and T. Y. Wu, *Ind. Eng. Chem. Res.*, **55**, 4363 (2016).
14. L. Yan, Y. Wang, J. Li, H. Ma, H. Liu, T. Li and Y. Zhang, *Desalination*, **341**, 87 (2014).
15. F. Ferrag-Siagh, F. Fourcade, I. Soutrel, H. Aït-Amar, H. Djelal and A. Amrane, *J. Chem. Technol. Biotechnol.*, **88**, 1380 (2013).
16. N. Oturan, J. Wu, H. Zhang, V. K. Sharma and M. A. Oturan, *Appl. Catal. B: Environ.*, **140**, 92 (2013).
17. F. Duan, Y. Li, H. Cao, Y. Wang, J. C. Crittenden and Y. Zhang, *Chemosphere*, **125**, 205 (2015).
18. R. Daghrir, P. Drogui and J. Tshibangu, *Sep. Purif. Technol.*, **131**, 79 (2014).
19. S. Zheng, F. Yang, S. Chen, L. Liu, Q. Xiong, T. Yu, F. Zhao, U. Schröder and H. Hou, *J. Power Sources*, **284**, 252 (2015).
20. E. Yuksel, M. Eyvaz and E. Gurbulak, *Environ. Prog. Sustain. Energy*, **32**, 60 (2013).
21. S. Pulkka, M. Martikainen, A. Bhatnagar and M. Sillanpää, *Sep. Purif. Technol.*, **132**, 252 (2014).
22. E. Brillas and I. Sirés, *TrAC Trends in Analytical Chemistry*, **70**, 112 (2015).
23. F. Gerayeli, F. Ghojavand, S. M. Mousavi, S. Yaghmaei and F. Amiri, *Sep. Purif. Technol.*, **118**, 151 (2013).
24. K. M. Sharif, M. M. Rahman, J. Azmir, A. Mohamed, M. A. Jahurul, F. Sahena and I. S. M. Zaidul, *J. Food Eng.*, **124**, 105 (2014).
25. W. H. Wong, W. X. Lee, R. N. Ramanan, L. H. Tee, K. W. Kong, C. M. Galanakis, J. Sun and K. N. Prasad, *Ind. Crop. Prod.*, **63**, 238 (2015).
26. C. Huyskens, J. Helsen and A. de Haan, *Desalination*, **328**, 8 (2013).
27. T. Y. Wu, A. W. Mohammad and N. Anuar, *J. Chem. Technol. Biotechnol.*, **84**, 1390 (2009).
28. K. P. Y. Shak and T. Y. Wu, *Ind. Crop. Prod.*, **76**, 1169 (2015).
29. M. R. Samarghandi, M. Khiadani, M. Foroughi and H. Z. Nasab, *Environ. Sci. Pollut. Res.*, **23**, 887 (2016).
30. M. N. Sepehr, K. Yetilmezsoy, S. Marofi, M. Zarrabi, H. R. Ghaffari, M. Fingas and M. Foroughi, *J. Taiwan Inst. Chem. Eng.*, **45**, 2786 (2014).
31. R. Shokoohi, G. Asgari, M. Leili, M. Khiadani, M. Foroughi and M. S. Hemmat, *Int. J. Environ. Sci. Technol.*, **14**, 841 (2017).
32. L. Zhang, X. Song, X. Liu, L. Yang, F. Pan and J. Lv, *Chem. Eng. J.*, **178**, 26 (2011).
33. T. Yehya, M. Chafi, W. Balla, C. Vial, A. Essadki and B. Gourich, *Sep. Purif. Technol.*, **132**, 644 (2014).
34. M. Khiadani, M. Foroughi and M. M. Amin, *Desalin. Water Treat.*, **52**, 678 (2014).
35. P. Nidheesh and R. Gandhimathi, *Desalination*, **299**, 1 (2012).
36. T. Zheng, Q. Wang, Z. Shi, Y. Fang, S. Shi, J. Wang and C. Wu, *J. Environ. Sci.*, **50**, 21 (2016).
37. S. Benredouane, T. Berrama and N. Doufene, *Chemometr. Intell. Lab. Syst.*, **155**, 128 (2016).
38. C. David, M. Arivazhagan and F. Tuvakara, *Ecotoxicol. Environ. Saf.*, **121**, 142 (2015).
39. K. Govindan, M. Noel and R. Mohan, *J. Water Process Eng.*, **6**, 58 (2015).
40. E. Henry Ezechi, M. H. Isa, S. R. bin Mohamed Kutty and Z. Ahmed, *J. Environ. Chem. Eng.*, **3**, 1962 (2015).
41. Y. S. Jeon, J. S. Yang, E. R. Park, J. W. Yang and K. Baek, *J. Taiwan Inst. Chem. Eng.*, **64**, 142 (2016).
42. E. E. Gerek, S. Yilmaz, A. S. Koparal, Ö. N. Gerek, *J. Water Process Eng.*, (2017) (In Press, Corrected Proof).
43. T. I. Liakos, S. Sotiropoulos and N. K. Lazaridis, *J. Environ. Chem. Eng.*, **5**, 699 (2017).
44. Y. Long, H. Li, X. Xing and J. Ni, *Chem. Eng. J.*, **325**, 360 (2017).
45. C. Zhang, Y. Jiang, Y. Li, Z. Hu, L. Zhou and M. Zhou, *Chem. Eng. J.*, **228**, 455 (2013).
46. B. Kakavandi, A. Takdastan, N. Jaafarzadeh, M. Azizi, A. Mirzaei and A. Azari, *J. Photochem. Photobiol. A Chem.*, **314**, 178 (2016).

47. Design Expert Software, In: Trial Version 8.0.7.1 User's Guide (2011).
48. E. A. Okogbenin, O. B. Okogbenin, J. U. Obibuzor and A. O. Emoghene, *Int. J. Stat. Appl.*, **4**, 117 (2014).
49. Eigenvector Documentation Wiki (2014), Half-normal probability plot, http://wiki.eigenvector.com/index.php?title=Half-Normal_Probability_Plot. Accessed in July 2017.
50. Y. N. Dholariya, Y. B. Bansod, R. M. Vora, S. S. Mittal, A. E. Shirsat and C. L. Bhingare, *Int. J. Pharm. Investig.*, **4**, 93 (2014).
51. T. González, J. R. Domínguez, P. Palo, J. Sánchez-Martín and E. M. Cuerda-Correa, *Desalination*, **280**, 197 (2011).
52. V. T. Banala, B. Srinivasan, D. Rajamanickam, B. Basappa Veerbadraiah and M. Varadarajan, *ISRN Pharmaceutics*, 1 (2013).
53. K. Yetilmezsoy, S. Demirel and R. J. Vanderbei, *J. Hazard. Mater.*, **171**, 551 (2009).
54. H. Zhang, Y. Li, X. Wu, Y. Zhang and D. Zhang, *Waste Manage.*, **30**, 2096 (2010).
55. Minitab I. MINITAB Release 17: Statistical Software for Windows. Minitab Inc., U.S.A. (2014).
56. B. Gomez-Ruiz, S. Gómez-Lavín, N. Diban, V. Boiteux, A. Colin, X. Dauchy and A. Urtiaga, *Chem. Eng. J.*, **322**, 196 (2017).
57. C. Comninellis, M. Doyle and J. Winnick (Eds.), Energy and electrochemical processes for a cleaner environment, In: Proceedings of the International Symposium held during the 2001 Joint International Meeting of the ECS and ISE in San Francisco, California, U.S.A. (2001).
58. S. Wilson, W. Farone, G. Leonard, J. Birnstingl and A. Leombruni, Catalyzed persulfate: advancing in situ chemical oxidation (ISCO) technology, Regenesis Bioremediation Products Inc., San Clemente, CA, U.S.A. (2013).
59. M. S. Diallo, N. A. Fromer and M. S. Jhon (Eds.), Nanotechnology for sustainable development. Springer Science & Business, New York, U.S.A. (2014).
60. T. Yehya, M. Chafi, W. Balla, C. Vial, A. Essadki and B. Gourich, *Sep. Purif. Technol.*, **132**, 644 (2014).
61. J. Wisniak, S. Stefanovic, E. Rubin, Z. Hoffman and Y. Talmon, *J. Am. Oil Chem. Soc.*, **48**, 379 (1971).
62. P. Asaithambi, M. Susree, R. Saravanathamizhan and M. Matheswaran, *Desalination*, **297**, 1 (2012).
63. V. Khandegar and A. K. Saroha, *Chin. J. Chem. Eng.*, **20**, 439 (2012).
64. W. Can, H. Yao-Kun, Z. Qing and J. Min, *Chem. Eng. J.*, **243**, 1 (2014).
65. I. Yahiaoui, F. Aissani-Benissad, F. Fourcade and A. Amrane, *Chem. Eng. J.*, **221**, 418 (2013).

# Supporting Information

# Electrodegradation of tetracycline using stainless steel net electrodes: Screening of main effective parameters and interactions by means of a two-level factorial design

**Maryam Foroughi\*, Hamid Reza Soheil Arezoomand\*, Ali Reza Rahmani\*\*, Ghorban Asgari\*\*\*, Davood Nematollahi\*\*\*\*, Kaan Yetilmezsoy\*\*\*\*\*, and Mohammad Reza Samarghandi\*,†**

\*Department of Environmental Health Engineering, School of Health,
Hamadan University of Medical Sciences, Hamadan, Iran
\*\*Department of Environmental Health Engineering & Research Centre for Health Sciences,
School of Public Health, Hamadan University of Medical Sciences, Hamadan, Iran
\*\*\*Social Determinants of Health Research Center (SDHRC), Faculty of Public Health,
Department of Environmental Health Engineering, Hamadan University of Medical Sciences, Hamadan, Iran
\*\*\*\*Faculty of Chemistry, Bu-Ali-Sina University, Hamadan, Iran
\*\*\*\*\*Department of Environmental Engineering, Faculty of Civil Engineering,
Yildiz Technical University, Davutpasa Campus, 34220, Esenler, Istanbul, Turkey
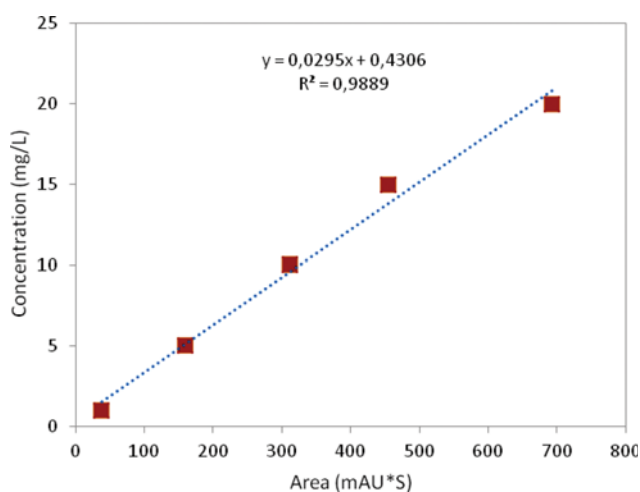
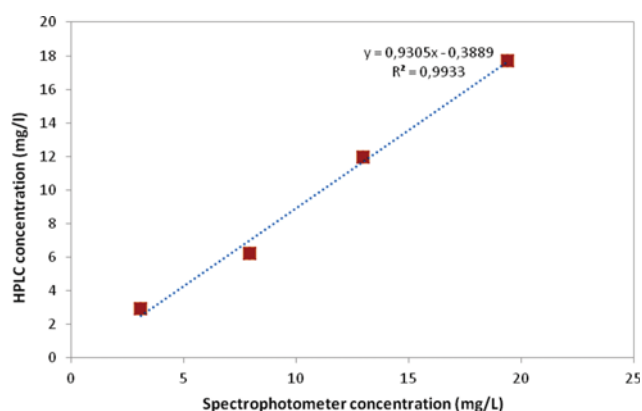Fig. S1. HPLC calibration curve.
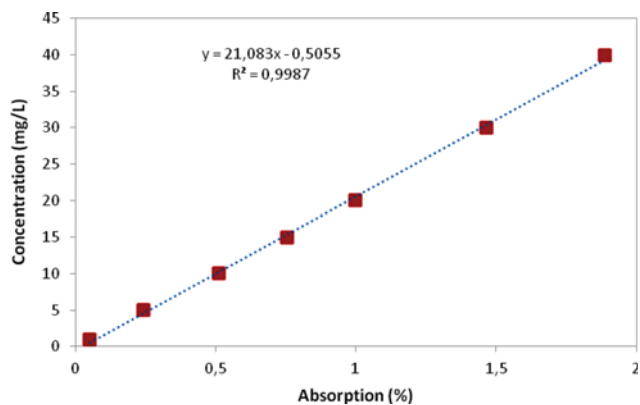


Fig. S3. Correlation between HPLC and spectrophotometer concentrations.



Fig. S2. Spectrophotometer calibration curve.